INVENTORY OF SUPPLEMENTAL INFORMATION

Supplemental Figures

Supplemental Movies

Supplemental Experimental Procedures

Supplemental References

SUPPLEMENTAL FIGURES

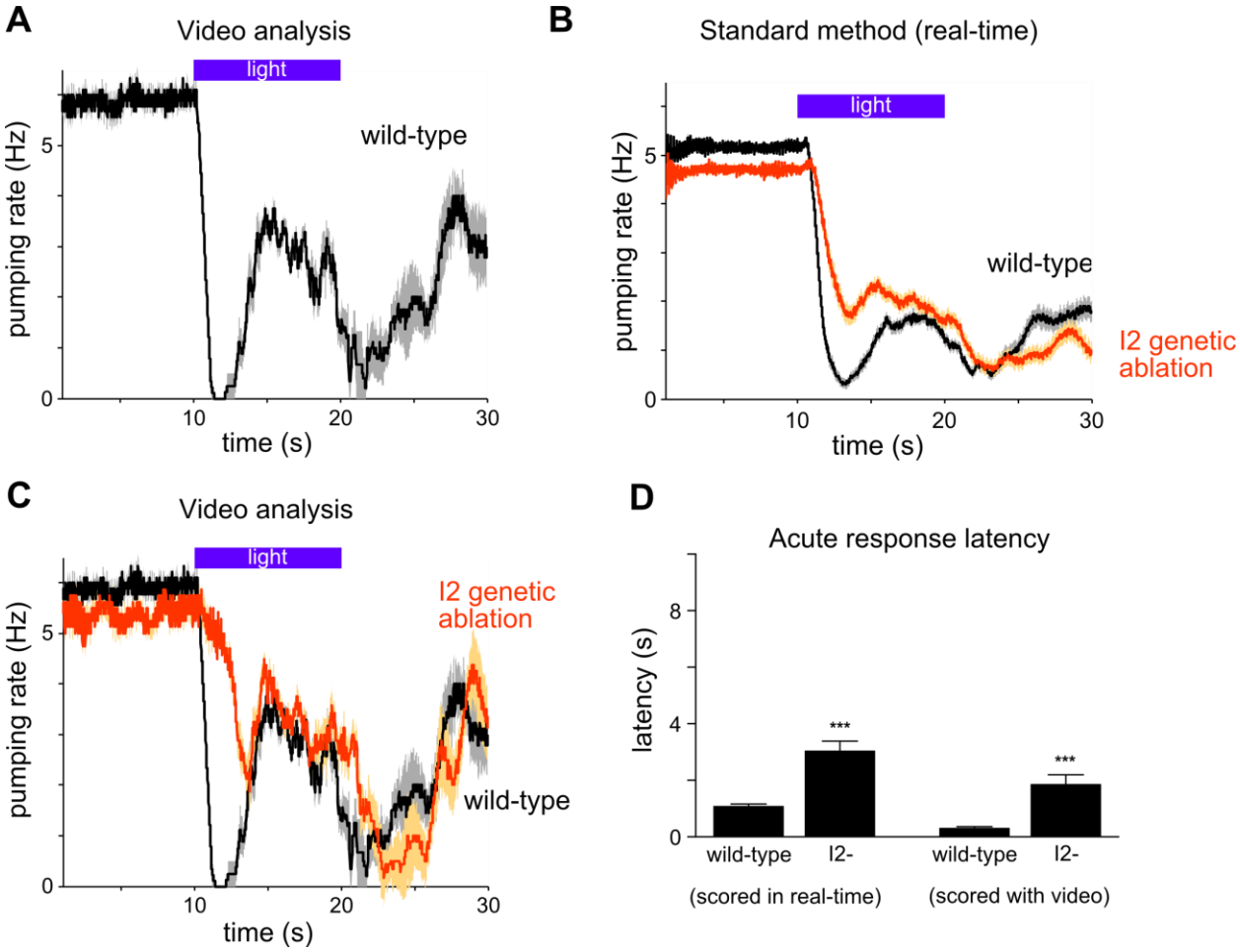

Figure S1, related to Figures 1 and 3. Video confirmation of real-time pumping measurements.

(A) Pumping response to light of wild-type animals scored by reviewing high-frame rate video (86 fps). The acute, burst and recovery phases of the response are visible. n = 9 worms.
(B) Genetic ablation of the I2 neurons by expression of the transgene *flp-15*$_{prom}$*::csp-1b* caused an acute response defect similar to that observed after I2 laser ablation (Figure 3B). These worms were scored by eye in real-time. n = 60 worms.
(C) Pumping response to light of I2-ablated animals (*flp-15*$_{prom}$*::csp-1b*) scored by reviewing high-frame-rate video. The acute response defect is similar to that in (b). n = 8 worms.
(D) Quantification of the acute response latency for the wild type and I2 genetic ablation by eye and by video analysis.

Shading around traces and error bars indicate s.e.m. *** $p < 0.001$, t-test compared to the corresponding wild-type.

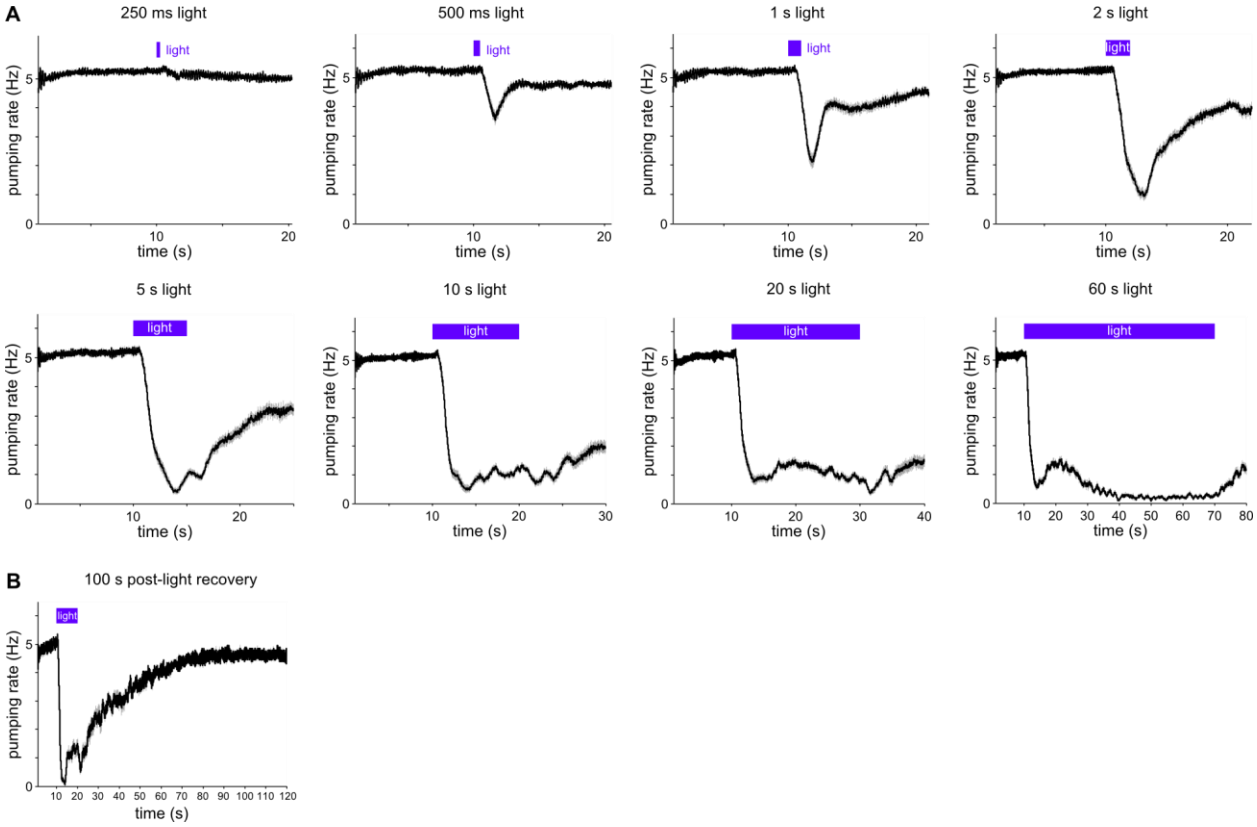

Figure S2, related to Figure 1. **Varying the duration of light exposure and the recovery period.**

(A) Pumping response to light for durations of 0.25-60 s. n = 60 worms.
(B) Pumping response observed for 100 s after light removal. Worms fully recovered to baseline pumping rates after 68 s. n = 20 worms.

Shading around traces and error bars indicate s.e.m.

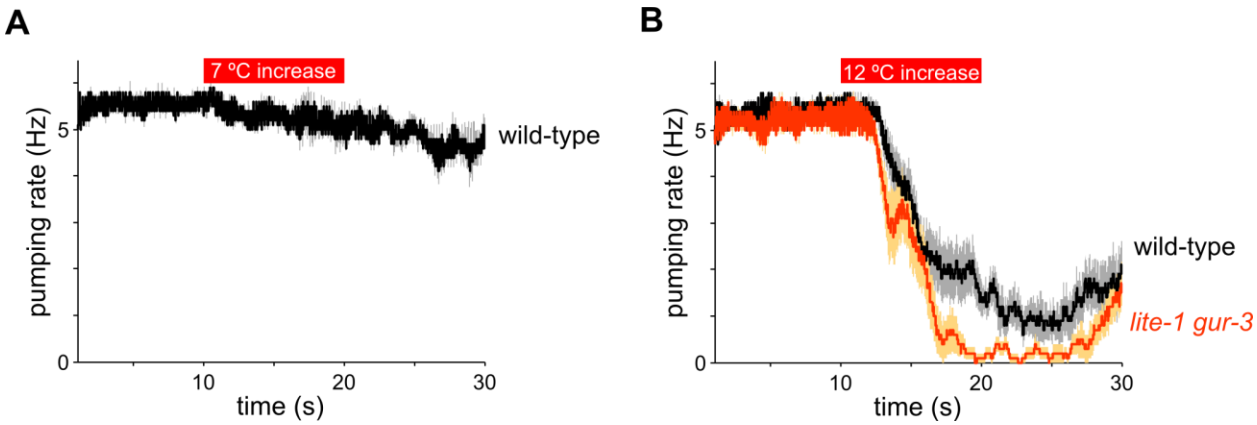

Figure S3, related to Figure 1. A temperature increase significantly beyond that generated by light inhibits pumping independent of *lite-1* and *gur-3*.

(A) A temperature increase of 7 °C from room temperature (22-23 °C) did not inhibit pumping in the wild-type. For comparison, light caused a temperature increase of 1-2.1 °C.
(B) A temperature increase of 12 °C from room temperature inhibited pumping in the wild type as well as the *lite-1 gur-3* double mutant.

n = 10 worms. Shading around traces and error bars indicate s.e.m.

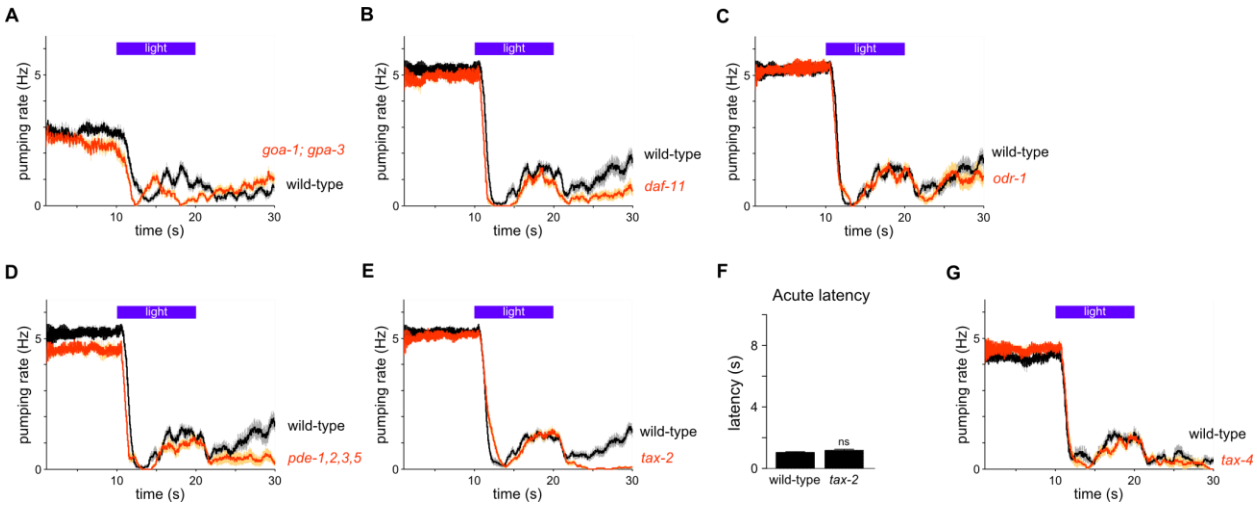

Figure S4, related to Figure 2. Mutants defective in genes that function downstream of *lite-1* exhibit a normal acute response to light.

(A) Mutants of the G proteins *goa-1(n1134); gpa-3(pk35)* did not have a defective acute response.
(B) Mutants of the guanylyl cyclase *daf-11(m47)* had a normal acute response.
(C) Mutants of the guanylyl cyclase *odr-1(n1936)* had a normal acute response.
(D) Mutants of the phosphodiesterases *pde-1(nj57),2(tm3098),3(nj59),5(nj49)* had a normal acute response.
(E) Mutants of the cGMP-gated ion channel *tax-2(p671)* had a slight latency defect, but that defect was not significant.
(F) Quantification of the acute response latency of *tax-2* mutants.
(G) Mutants of the cGMP-gated ion channel *tax-4(p678)* had a normal acute response.

n = 20-40 worms. Shading around traces and error bars indicate s.e.m. ns = not significant, t-test compared to wild-type.

Figure S5

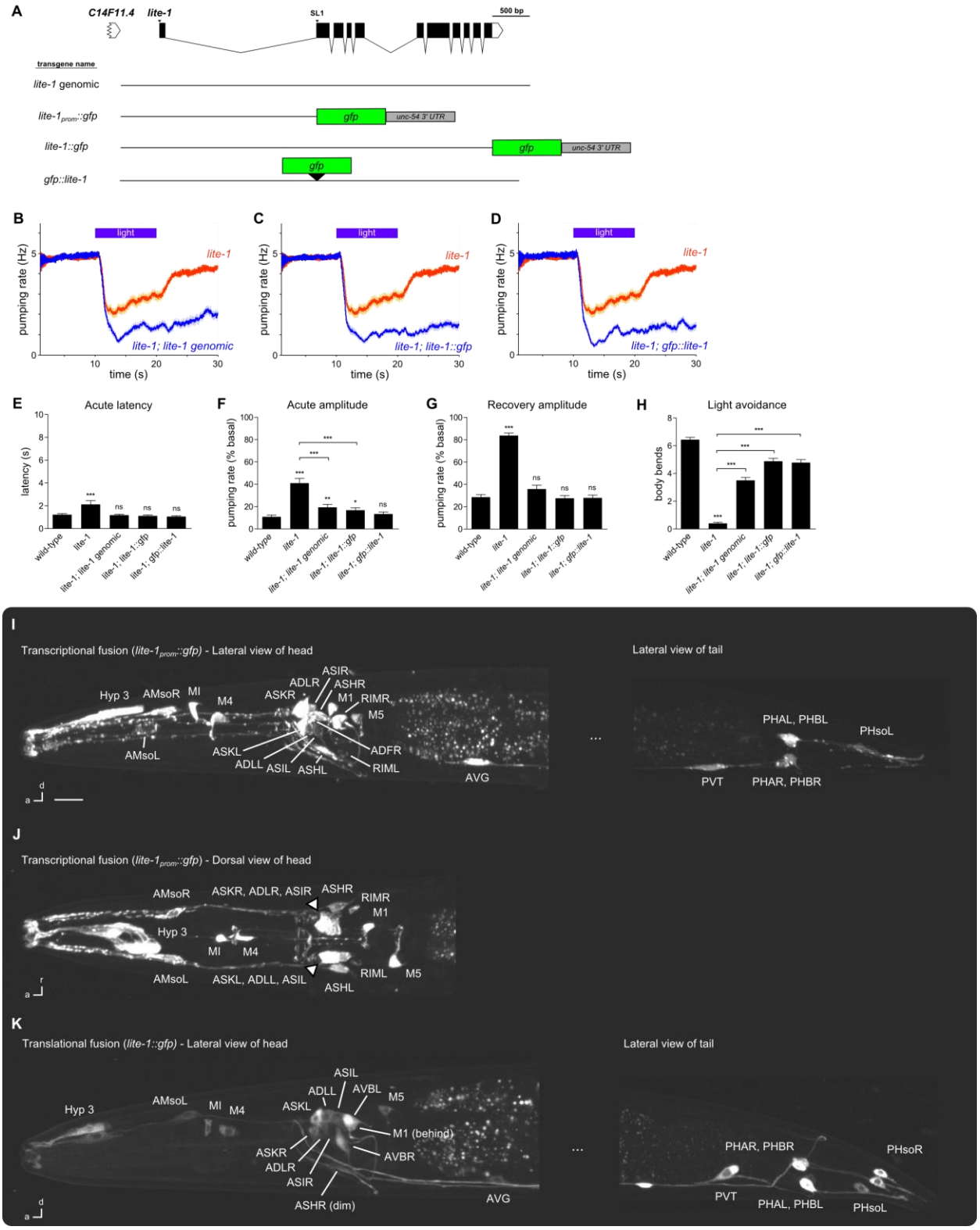
A
C14F11.4
lite-1
SL1
500 bp
transgene name
lite-1 genomic
lite-1prom::gfp
gfp
unc-54 3' UTR
lite-1::gfp
gfp::lite-1
B
C
D
light
pumping rate (Hz)
time (s)
lite-1
lite-1; lite-1 genomic
lite-1; lite-1::gfp
lite-1; gfp::lite-1
E
Acute latency
latency (s)
F
Acute amplitude
pumping rate (% basal)
G
Recovery amplitude
H
Light avoidance
body bends
wild-type
lite-1
lite-1; lite-1 genomic
lite-1; lite-1::gfp
lite-1; gfp::lite-1
I
Transcriptional fusion (lite-1prom::gfp) - Lateral view of head
Lateral view of tail
Hyp 3
AMsoR
MI
M4
ASKR
ASIR
ADLR
ASHR
M1
RIMR
M5
AMsoL
ASKL
ADLL
ASIL
ASHL
ADFR
RIML
AVG
PHAL, PHBL
PHsoL
PVT
PHAR, PHBR
J
Transcriptional fusion (lite-1prom::gfp) - Dorsal view of head
AMsoR
ASKR, ADLR, ASIR
ASHR
RIMR
M1
Hyp 3
MI
M4
AMsoL
ASKL, ADLL, ASIL
ASHL
RIML
M5
K
Translational fusion (lite-1::gfp) - Lateral view of head
Lateral view of tail
Hyp 3
AMsoL
MI
M4
ASIL
ADLL
AVBL
M5
ASKL
M1 (behind)
ASKR
AVBR
ADLR
ASIR
ASHR (dim)
AVG
PHAR, PHBR
PHsoR
PVT
PHAL, PHBL
PHsoL

Figure S5, related to Figure 2. *lite-1* expression rescues the defects of *lite-1* mutants, and *lite-1* is expressed in 29 cells.

(A) The *lite-1* gene, showing the design of several *lite-1* transgenes. The *lite-1* gene model was semi-automatically constructed using the Exon-Intron Graphic Maker (available at http://www.wormweb.org).
(B) The *lite-1* genomic locus rescued the pumping inhibition defect of *lite-1(ce314)* mutants.
(C) The *lite-1*$_{prom}$*::lite-1::gfp* transgene rescued the pumping inhibition defect of *lite-1* mutants.
(D) The *lite-1*$_{prom}$*::gfp::lite-1* transgene rescued the pumping inhibition defect of *lite-1* mutants.
(E) Quantification of acute response latency.
(F) Quantification of acute response amplitude.
(G) Quantification of recovery response amplitude.
(H) Strains carrying all three *lite-1* transgenes were rescued for the light avoidance defect of *lite-1* mutants. Body bends were scored during 10 s of light exposure.
(I) Expression pattern of the transcriptional fusion (*lite-1*$_{prom}$*::gfp*) in the adult head and tail. No expression was observed in the midbody.
(J) Dorsal view of the transcriptional fusion expression pattern in the adult head.
(K) Expression pattern of the C-terminal translational fusion (*lite-1*$_{prom}$*::lite-1::gfp*) in the adult head and tail. No expression was observed in the midbody.

For behavioral assays, n = 60 worms. Shading around traces and error bars indicate s.e.m. * $p < 0.05$, ** $p < 0.01$, *** $p < 0.001$, ns = not significant, t-test, compared to the wild type or to the strain indicated. d = dorsal, a = anterior, r = right. Scale bars, 8 µm.

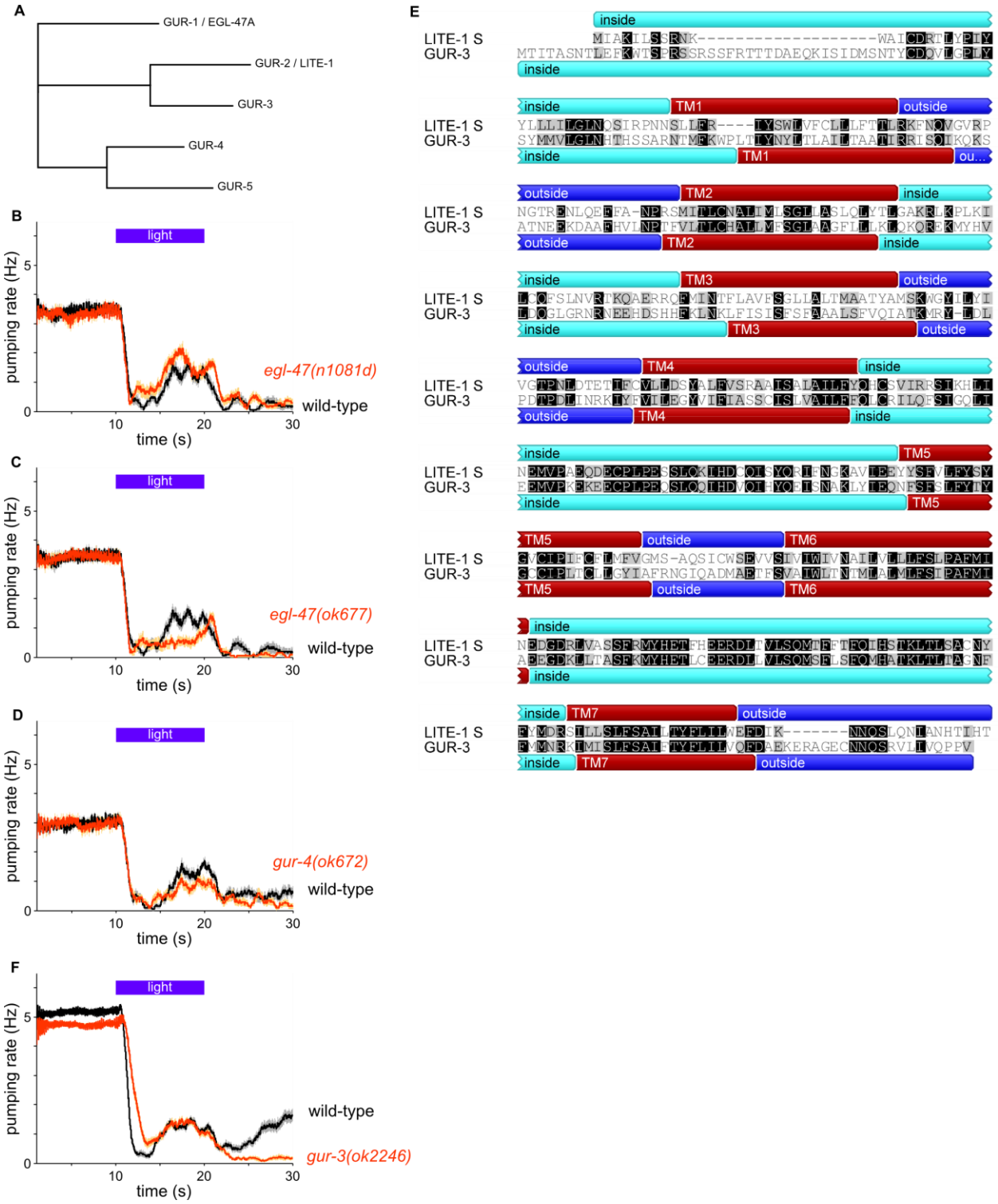

Figure S6, related to Figure 3. The gustatory receptor family in *C. elegans*.

(A) Five paralogs of the *Drosophila* gustatory receptor family are present in the worm genome. The tree was generated using Geneious (Biomatters).
(B) *egl-47(n1081d)* mutants did not exhibit a defect in the pumping response to light.

(C) *egl-47(ok677)* mutants did not exhibit a defect in the pumping response to light.
(D) *gur-4(ok672)* mutants did not exhibit a defect in the pumping response to light.
(E) Alignment between LITE-1S and GUR-3. LITE-1S and GUR-3 are 41% identical The alignment was generated using ClustalW. A black box indicates amino acid identity, and a grey box indicates amino acid similarity, as defined by a Blosum55 score matrix with a threshold of 1. Amino acid sequences are from WormBase. LITE-1S is described in (Liu et al., 2010). Transmembrane predictions are from TMHMM (http://www.cbs.dtu.dk/services/TMHMM/).
(F) *gur-3(ok2246)* mutants exhibited a defect in the acute response to light like *gur-3(ok2245)* mutants (Figure 2B).

$n \geq 20$ worms. Shading around traces and error bars indicate s.e.m.

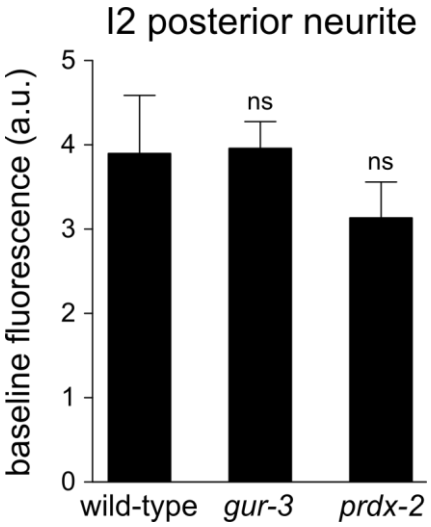

Figure S7, related to Figures 4 and 7. *gur-3* and *prdx-2* mutants exhibit baseline GCaMP3 fluorescence in their I2 neurons similar to that of the wild type.

The posterior neurite of I2 was analyzed. $n \geq 22$ worms. Error bars indicate s.e.m, a.u. = arbitrary units, ns = not significant, t-test compared to wild-type.

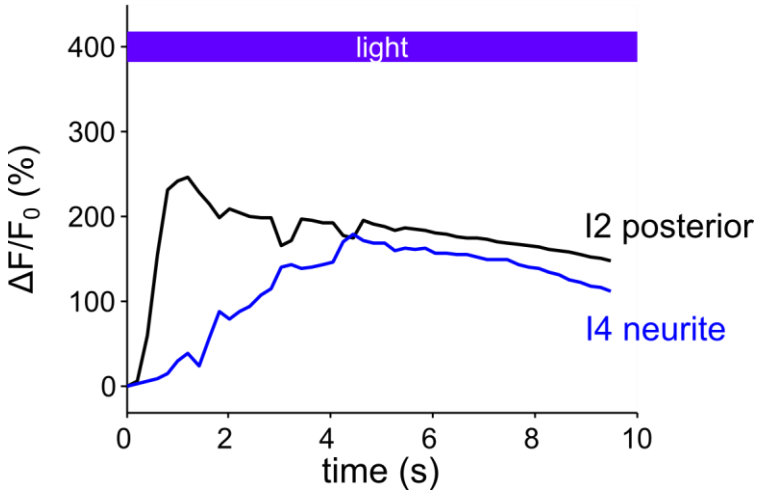

Figure S8, related to Figure 4. The I4 neuron, which expresses *gur-3*, responds to light.

Calcium imaging of a worm carrying *gur-3*$_{prom}$*::gcamp3*. Black line is the response to light in the I2 posterior neurite. Blue line is the response to light in the I4 neurite. n = 1.

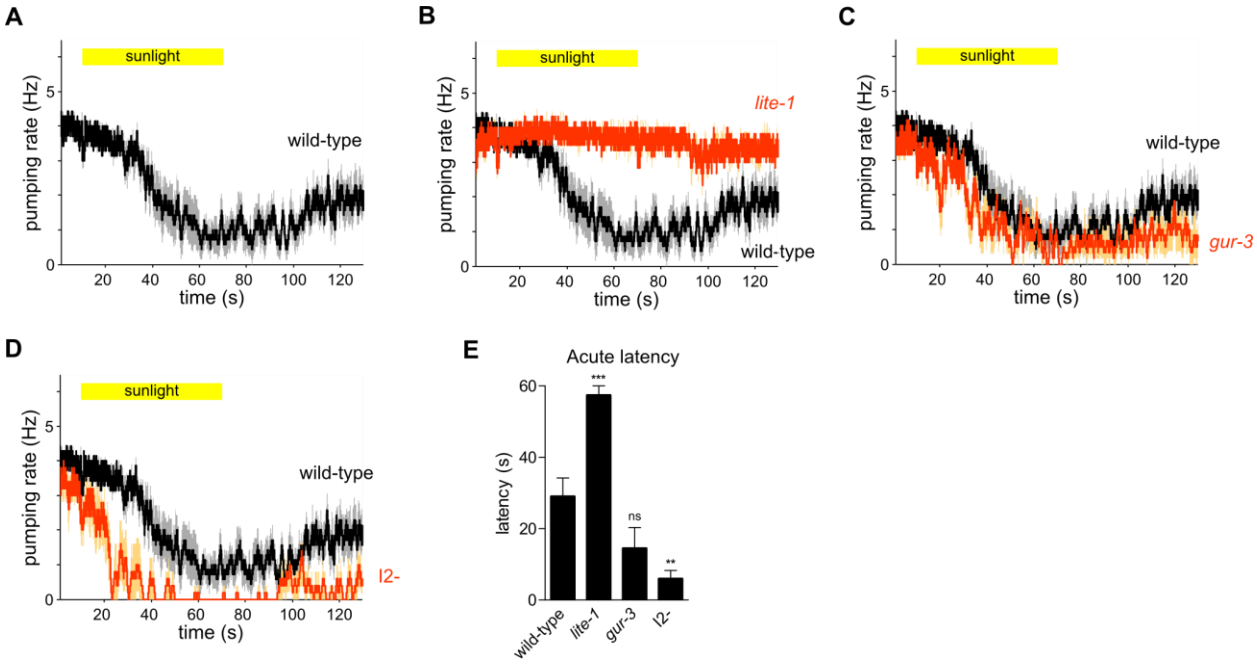

Figure S9, related to Figure 5. Sunlight inhibits feeding in a *lite-1*-dependent manner.

(A) Pumping of wild-type worms was inhibited by exposure to sunlight. n = 7 worms.
(B) Pumping of *lite-1* mutants was not inhibited by exposure to sunlight. n = 6 worms.
(C) Pumping of *gur-3* mutants was inhibited by exposure to sunlight. n = 6 worms.
(D) Pumping of animals lacking the I2 neurons due to genetic ablation was inhibited by exposure to sunlight. n = 5 worms.
(E) Quantification of acute response latency.

Shading around traces and error bars indicate s.e.m. ** $p < 0.01$, *** $p < 0.001$, ns = not significant, t-test compared to wild-type.

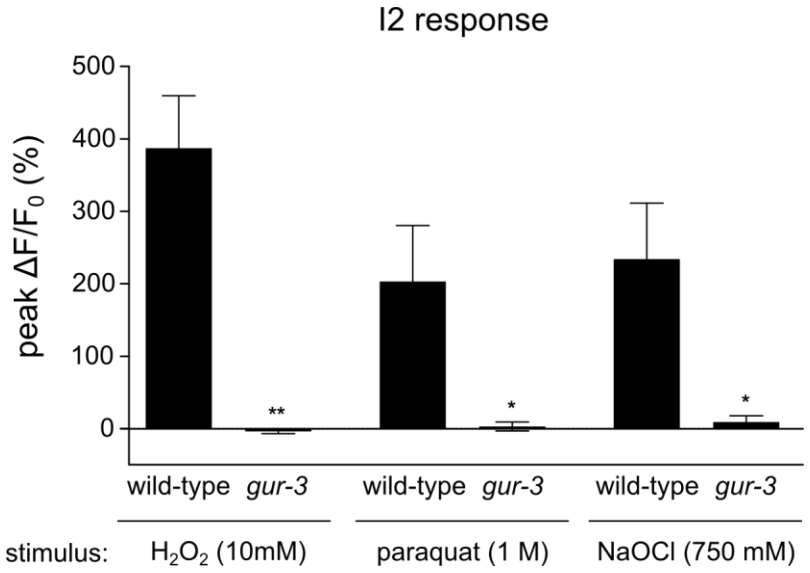

Figure S10, related to Figure 6. Paraquat and sodium hypochlorite activate I2 via *gur-3*.

Response in the I2 soma. n = 5 cells. * $p < 0.05$, ** $p < 0.01$, t-test compared to corresponding wild-type animals.

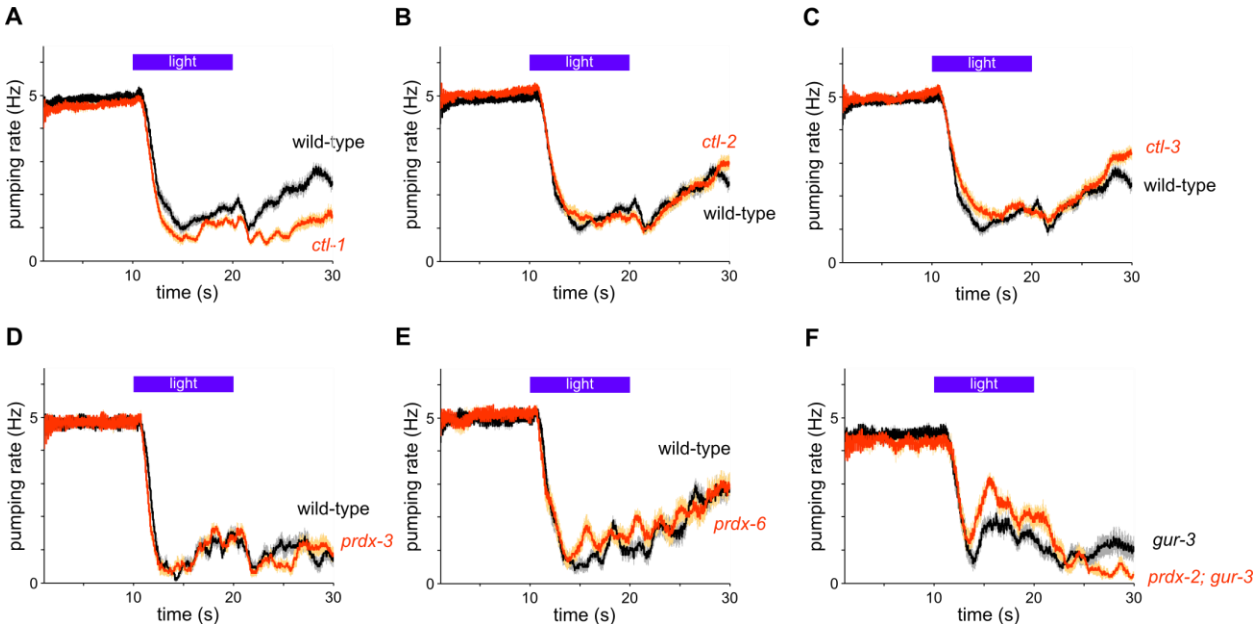

Figure S11, related to Figure 7. Catalases and peroxiredoxins other than *prdx-2* are not required for the pumping response to light.

(A) *ctl-1(ok1242)* mutants exhibited a normal acute pumping response to light.
(B) *ctl-2(ok1137)* mutants exhibited a normal pumping response to light.
(C) *ctl-3(ok2042)* mutants exhibited a normal pumping response to light.
(D) *prdx-3(gk529)* mutants exhibited a normal pumping response to light.
(E) *prdx-6(tm4225)* mutants exhibited a normal pumping response to light.
(F) *prdx-2(gk169); gur-3(ok2245)* double mutants exhibited an acute response defect similar to that of *gur-3(ok2245)* single mutants.

$n \geq 20$ worms. Shading around traces and error bars indicate s.e.m. For (A-C), light power used was 4.5 mW/mm^2 at 436 nm instead of the standard 13 mW/mm^2.

SUPPLEMENTAL MOVIES

Movie S1, related to Figure 1. *C. elegans* inhibits pumping in response to light.
Video of worm taken using a 20x objective. White square indicates the moment violet light (400 nm, 8 mW/mm^2, 2 s) was projected onto the field of view. Video was slowed to ¼ real-time, 5 fps, 20 s total duration.

Movie S2, related to Figure 4. The I2 neuron responds to light.
Video of transgenic worm carrying *flp-15$_{prom}$::gcamp3* taken using a 40x air objective. Blue light (485 nm, 26 mW/mm^2) was projected onto the field of view during the entire duration (7 s). Video playback is real-time, 15 fps. 485 nm light was used instead of 436 nm light to allow simultaneous calcium imaging and light stimulation.

SUPPLEMENTAL EXPERIMENTAL PROCEDURES

Strains

The following worm strains were used:

N2 (the wild type)
MT20722 *lite-1(ce314)*
MT20515 *goa-1(n1134); gpa-3(pk35)*
MT4589 *odr-1(n1936)*
DR47 *daf-11(m47)*
TQ1828 *pde-1(nj57) pde-5(nj49); pde-3(nj59); pde-2(tm3098)*
PR671 *tax-2(p671)*
PR678 *tax-4(p678)*
MT23117 *lite-1(ce314) lin-15(n765); nEx2275[lite-1 genomic, lin-15(+)]*
MT23127 *lin-15(n765); nEx2285[lite-1$_{prom}$::gfp, lin-15(+)]*
MT23123 *lite-1(ce314) lin-15(n765); nEx2281[lite-1$_{prom}$::lite-1::gfp, lin-15(+)]*
MT23121 *lite-1(ce314) lin-15(n765); nEx2279[lite-1$_{prom}$::gfp::lite-1; lin-15(+)]*
MT2248 *egl-47(n1081)*
RB845 *gur-4(ok672)*
MT21783 *gur-3(ok2245)*
RB1756 *gur-3(ok2246)*
MT21793 *lite-1(ce314) gur-3(ok2245)*
MT21910 *lin-15(n765); nEx2065[gur-3$_{prom}$::gfp, lin-15(+)]*
MT21421 *nIs569[flp-15$_{prom}$::csp-1b cDNA, ges-1$_{prom}$::gfp]*
MT21791 *lite-1(ce314) nIs569*
MT21790 *gur-3(ok2245) nIs569*
MT22166 *gur-3(ok2245) lin-15(n765); nEx2144[flp-15$_{prom}$::mCherry::gur-3, lin-15(+)]*
MT21650 *nIs575[flp-15$_{prom}$::gcamp3, lin-15(+)]; lin-15(n765)*
MT21785 *nIs575; gur-3(ok2245) lin-15(n765)*
MT22201 *nIs575; gur-3(ok2245) lin-15(n765); nEx2173[flp-15$_{prom}$::mCherry::gur-3, unc-122$_{prom}$::dsRed]*
MT21570 *nIs575; lite-1(ce314) lin-15(n765)*
MT23144 *lin-15(n765); nEx2298[gur-3$_{prom}$::gcamp3, lin-15(+)]*
MT21216 *lin-15(n765); nIs534[odr-1$_{prom}$::gcamp3, lin-15(+)]*
MT23160 *lin-15(n765); nIs534; nEx2314[odr-1$_{prom}$::gur-3, ges-1$_{prom}$::gfp]*
CX7376 *kyIs511[gcy-36$_{prom}$::gcamp, unc-122$_{prom}$::gfp]*
MT23162 *kyIs511; nEx2316[gcy-36$_{prom}$::gur-3, ges-1$_{prom}$::gfp]*
MT23129 *lin-15(n765); nEx2287[egl-6a$_{prom}$::gur-3, lin-15(+)]*
MT23114 *lin-15(n7765); nEx2272[myo-3$_{prom}$::gur-3, lin-15(+)]*
RB1197 *ctl-1(ok1242)*
VC754 *ctl-2(ok1137)*
RB1653 *ctl-3(ok2042)*
VC1151 *prdx-3(gk529)*
FX04225 *prdx-6(tm4225)*
VC289 *prdx-2(gk169)*

MT21898 *prdx-2(gk169); lite-1(ce314)*
MT21927 *prdx-2(gk169); lin-15(n765); nEx2078[prdx-2$_{prom}$::prdx-2::mCherry, lin-15(+)]*
MT22177 *prdx-2(gk169); lin-15(n765); nEx2155[flp-15$_{prom}$::prdx-2 cDNA, lin-15(+)]*
MT21899 *prdx-2(gk169); nIs575; lin-15(n765)*
MT22186 *prdx-2(gk169); nIs575; lin-15; nEx2162[flp-15$_{prom}$::prdx-2 cDNA, P$_{unc-122}$::dsRed]*
MT22080 *prdx-2(gk169); gur-3(ok2245)*

Molecular biology

We used the following primers to amplify DNA for generating transgenes by standard cloning and PCR fusion procedures. For PCR fusion, the appropriate overlapping region was appended to these primers. For cDNA preparation, wild-type mixed-stage poly-A RNA was used as template.

lite-1 genomic:	CATCAACGGACGTCGTGATTCTC, CGGCAGTTTCAGTTGATGACAAAAAAATTG
lite-1$_{prom}$:	CAGCTAACATTTTGCTAACGCAGAAATATTAGG, GCAAATCGCCCATTTGTTACGACTC
lite-1$_{prom}$::lite-1:	CAGCTAACATTTTGCTAACGCAGAAATATTAGG, TGTGTGAATCGTGTGGTTTGCGATATTC
lite-1:	ATGATCGCAAAAATCCTGTCGAGTCG, GTAAATGCAACCCTAGCCACATGC
gur-3$_{prom}$:	GCCTGATGGAACACACTTCCAAC, CAACGTATTCGACGCTGTTATCGTC
flp-15$_{prom}$:	TGAACTTTCCTCATTTCCCCTTCGTTC, GACGAGGTGTATGTGGGAGACC
csp-1b cDNA:	ATGCCGAGAACGGACGCC, TTACATCGACCTTGAAAAGTGCCAT
gur-3:	ATGACGATAACAGCGTCGAATACGTT, GTTTACCCCGTCTCTATTTCCGCTTTG
odr-1$_{prom}$:	TGGGTACAACAATTTCTCATTC, ATTGGCCTTCTGCTCAAA
gcy-36$_{prom}$:	GATATGATGTTGGTAGATGGGGTTTGG, CATTGTTGGGTAGCCCTTGTTTGAATTTAC
egl-6$_{prom}$:	CCCTTTGATCAACATTTCATCCTTTTTTGTTTG, TGTGTTCTATGATGTTCTCCATCTGCAAC
prdx-2$_{prom}$::prdx-2:	TGAAGCATTTGCAAGAAAGCTCGAC, GTGCTTCTTGAAGTACTCTTGGCTTTC
prdx-2 cDNA:	ATGTCGAAAGCATTCATCGGAAAGC, CGGTTATCAAGCAATTTCATGAATTTCAGAATTTC

myo-3$_{prom}$*::gur-3* was cloned as described for *myo-3*$_{prom}$*::lite-1* (Edwards et al., 2008). The 3' UTR was from *unc-54* unless an endogenous UTR was present. The molecular lesion of *gur-3(ok2245)* was identified by Sanger sequencing. The deletion lies in the interval including GTAAGTTCACTGGAATGAAC to TGTTTCCTATTAGTATGGTG, which covers from the first base after the first exon to the 4th intron. The sequence TT is inserted in this interval. We used the following primers for genotyping (L = left, OL = outer left, IL = inner left, OR = outer right, IR = inner right):

gur-3(ok2245): L: ATGACGATAACAGCGTCGAATACGTT
OR: GAAACTAGTTCGTTTTTAGGAAATTGAGACTGTC
IR: CAAAAACCATGTATTCTTTGTGCGATTTTCATG
prdx-2(gk169): OL: CATGTCTCTCGCTCCAAAGGTGC
OR: GTGATGGGTCGATGATGAAGAGTCC
IL: CGCTCTCCAATTTTGCCAATGTATTTC
IR: GCCTTGAACTCCTCAGCACGG

Behavioral response to light

Worms were maintained at 20 °C. 40-80 larval stage 4 (L4) or young adult worms were picked on day 1 to a 6 cm Petri dish filled with nematode growth medium (NGM) agar seeded with OP50 *E. coli* bacteria (Brenner, 1974). Worms were assayed on day 2 at 22.5 °C or room temperature and were scored non-blind to experimental condition. For the response to light, pumping was scored by eye using a stereo dissecting microscope set to 120x magnification and illuminated with a halogen transmitted light source (Zeiss Lumar and KL 2500 LCD, 3100 K). Custom Matlab software (available at http://www.wormweb.org) recorded the timing of pumps as indicated by manual key presses and controlled a shutter (via Zeiss EMS-1 controller) that presented and removed mercury arc epi-illumination (HBO 100). The epi-illumination irradiated the entire worm with a spot diameter of approximately 2 mm. The standard assay began with a baseline period of 10 s, followed by 10 s of arc illumination, followed by 10 s without arc

illumination. We used a modified CFP filter set (Zeiss Lumar 47 HE CFP 486047) to illuminate 436 ± 13 nm violet light at an intensity of 13 mW/mm^2, and we observed pumping with a long-pass GFP emission filter. Each worm was tested once, except in ablation experiments in which each worm was assayed 1-4 times with several minutes allowed for recovery between assays. To test responses to sunlight, we took the worms outside on a clear, sunny day in the month of October (13-16 °C). The sun's intensity was measured to be 0.005-0.006 mW/mm^2 from 359-370 nm, similar to the ASTM G17303 global tilt reference (Reference Solar Spectral Irradiance) of 0.008 mW/mm^2. At the start of the assay, the dissecting microscope was oriented so that the optics mounting pole cast a shadow on the worm. After 10 s the microscope was rotated so that the worm was exposed to direct sunlight for 60 s. Then the microscope was rotated back to the shadow position for the remaining 60 s. To assess the spectral sensitivity of the pumping response, worms were placed on an NGM agar pad on a coverslip and observed using an inverted microscope with a 20x air objective (Zeiss Axiovert S 100). Monochromatic arc illumination emitted 350, 400, 450, 500, and 550 ± 8 nm light onto the worms, and intensity was varied (Till Photonics Polychrome V, 150 W xenon bulb). A custom dichroic mirror was manufactured to reflect light across this range and transmit wavelengths greater than 600 nm (Chroma). Custom Matlab software controlled the Polychrome light source, and pumping was assayed by eye with the same protocol used with the dissecting microscope. Discrete pumping events were averaged using a 1 s backward moving average to generate average traces. Light power was measured using a laser power meter (Coherent FieldMate). Light avoidance was qualitatively scored if a worm either increased its speed or reversed in response to light.

For experiments in which *gur-3* was ectopically expressed in the HSN neurons (*egl-6a*$_{prom}$*::gur-3*) and body wall muscle (*myo-3*$_{prom}$*::gur-3*), 436 nm light was provided at 13

mW/mm^2 for 20 s, and egg-laying events and body bends were scored, respectively, during this time interval.

Behavioral response to heat

To measure the temperature change caused by exposure to the standard light (436 nm light, 13 mW/mm^2), a temperature sensor (Fluke 52 II thermocouple or Hanna Instruments Checktemp1) was placed on NGM agar and illuminated with light for 10 s. To expose worms to heat, hot air was blown (Tenma Hot Air Gun 21-11425) onto the agar surface such that a specific temperature increase would occur over 10 s, as measured with a temperature sensor. The hot air gun was set to 100 °C at the lowest flow rate setting and positioned 2-8 inches from the agar surface.

Behavioral response to hydrogen peroxide

Hydrogen peroxide generated by light was measured (WPI TBR 1025 with ISO-HPO-100 sensor) in the presence of 50 nM riboflavin and with or without 1000 U/ml catalase in M9. 15 ml of solution in a 6 cm Petri dish was exposed to 50 mW of 436 nm light using the same light source and power to which worms were exposed to in the standard light assay. The sensor was calibrated with known concentrations of hydrogen peroxide. The worm's pumping response to hydrogen peroxide vapor was scored in a manner similar to that used to score the pumping response to light. Pumping was scored by eye using the custom software described above. Hydrogen peroxide vapor was administered from a pulled glass needle loaded into a nanoliter injector (World Precision Instruments Nanoliter 2000, Micro4 controller). 30% hydrogen peroxide (8.82 M) was loaded into the needle. After 10 s, the needle was brought to the head of

the worm, and after 10 s, it was removed. For the behavioral response to hydrogen peroxide liquid, drops of varying concentrations (1 µM - 1 M) diluted in M9 were placed near the head of the worm while it was feeding on food. The drop flowed to cover part of the head such that hydrogen peroxide was sucked into the pharynx. The pumping response to hydrogen peroxide liquid was scored by observing whether pumping was inhibited in the following 10 s. The avoidance response to hydrogen peroxide liquid was scored as the number of smooth reversal body bends beginning immediately following the placement of the drop. All observations were made by eye using a macroscope (Wild Makroskop M420).

Behavioral statistics

For the pumping response, the acute response latency for a single trial is the time of the first missed pump relative to the onset of light. Notationally, t_i is the time of the i^{th} pump, l_i is the latency between the i^{th} and $i+1^{th}$ pump, and $\bar{l}$ is the mean latency for a set of pumps. To calculate the acute response latency, we calculated $\bar{l}_{pre-light}$ for the first 10 s prior to light onset and compared that to the latencies (l_j) observed during the following 10 s of light, in temporal order. For the first $l_j > 2\bar{l}_{pre-light}$, the acute response latency was calculated as

$$acute\ response\ latency = t_j - t_{light\ on} + \bar{l}_{pre-light}$$

where t_j is the time of the last pump with a pre-light latency and $t_{light\ on}$ is the time that light was turned on. The acute response amplitude is the rate of pumping in the first 3 s following the first missed pump normalized to the pre-light pumping rate. More formally, acute response amplitude was calculated as

$$acute\ response\ amplitude = \frac{n_{post-miss}/3}{n_{pre-light}/10}$$

where $n_{post-miss}$ is the number of pumps in the 3 s after the acute response latency after light onset and $n_{pre-light}$ is the number of pumps during the first 10 s of the experiment prior to light exposure. The recovery response amplitude is the rate of pumping in the 10 s following removal of light normalized to the pre-light pumping rate. The acute and recovery response amplitudes are reported as percentages.

Laser ablations

We used a pulsed nitrogen laser to conduct laser microsurgery of individual pharyngeal neurons (Laser Science, Inc. VSL-337 attached to a Zeiss Axioplan microscope) (Fang-Yen et al., 2012). The laser passed through a dye cell containing coumarin (5 mM in methanol), which shifted the wavelength from 337 nm to 435 nm. Worms were immobilized by 10 mM sodium azide and mounted on an agar pad between a coverslip and slide and examined through a 100x oil objective. Control animals experienced the same handling, except they were not exposed to the laser. Ablations were done using larvae of stage 1 or 2 (L1 or L2), and cells were identified based on nucleus location as observed by Nomarski differential interference contrast optics. Worms were placed on NGM plates following ablation for recovery. The next day, larvae were remounted to examine whether the intended ablation was successful. We confirmed that the cell either looked damaged, appeared as a refractile corpse, or was absent, compared to mock-ablated controls. On the following day, adults were assayed for their pumping or I2 calcium response to light by exposing them to bright violet light (436 nm, 13 mW/mm^2) or blue light (485 nm, 26 mW/mm2), respectively.

Calcium imaging

To study the calcium response of the I2 neuron, we generated a transgenic strain expressing GCaMP3 specifically in I2 and PHA, a neuron in the tail (*flp-15*$_{prom}$*::gcamp3*). To study the calcium response of the AWC and AWB neurons, we generated a transgenic strain expressing GCaMP3 under the *odr-1* promoter (*odr-1*$_{prom}$*::gcamp3*) with or without ectopic expression of *gur-3*. To study the calcium response in the URX neurons, we used an existing strain (*gcy-36*$_{prom}$*::gcamp* (Zimmer et al., 2009)) with or without ectopic expression of *gur-3*. To assay the response to light, worms were immobilized using the friction provided by 0.10 µm polystyrene beads (Polysciences, Inc. #00876) on 10% agarose in M9 (Kim et al., 2013). The slide was imaged using an inverted microscope (Zeiss Axiovert S 100) with a monochromatic xenon light source set to emit at 485 nm (Till Photonics Polychrome V). Via a 40x air objective, an electron multiplying charge coupled device (EMCCD) camera (Andor iXon+) recorded the changes in I2 or PHA fluorescence. In our standard assay, the worm was simultaneously imaged and stimulated with 26 mW/mm^2 485 nm light for 7 s, and videos were recorded at full resolution (1002x1004), 15 fps (temporal resolution of 66 ms), and 8-bit pixel depth. For AWC, AWB and URX calcium imaging, the protocol was modified so that worms were simultaneously imaged and stimulated with 10 mW/mm^2 485 nm light for 20 s, and videos were recorded at 2 fps. For the I2 spectral analysis, the power of 485 nm light was reduced (2 mW/mm^2) so that it failed to stimulate the I2 response. A specific wavelength was presented for 1 s, followed by low-power imaging light, which allowed us to record the response of I2 to different wavelengths.

To assay the response to hydrogen peroxide, worms were glued (Meridian Surgi-lock 2oc) to electrophysiological saline agarose pads (Goodman et al., 1998). The exposure time per frame was increased (100-200 ms, 1 fps). Worms were exposed to the vapor of 30% hydrogen

peroxide loaded into a glass needle, as described for the behavioral assay above. After 10 s, the needle was lowered near the nose of the worm, and after 10 s was removed. For liquid drop assays, 3 µl of liquid were dropped manually by pipette after 10 s, and remained for the remainder of the imaging period (50 s). All compounds were dissolved in distilled water.

To analyze some calcium-imaging videos, video frames were aligned using Fiji's StackReg plug-in. Videos were analyzed for changes in fluorescence in manually drawn regions of interest (ROIs) using a custom Matlab program. The fluorescence change in each compartment (anterior neurite, soma, posterior neurite) was calculated as

$$\frac{\Delta F}{F_0}(t) = \frac{F(t) - F_{bg}(t)}{F(0) - F_{bg}(0)} - 1$$

where F is the mean pixel value in an ROI and F_{bg} is the mean pixel value in a background ROI to control for bleaching. $\Delta F / F_0$ is represented as a percentage. Baseline fluorescence was calculated by subtracting the background fluorescence from the ROI in the first frame of light exposure, before the cell responded. For light and vapor experiments, the peak calcium response was the maximum value achieved during stimulus presentation. For liquid drop experiments, the peak calcium response was calculated by subtracting the peak fluorescence within an ROI in the first 10 s prior to liquid exposure from the peak fluorescence in the following 50 s during liquid exposure, divided by the peak fluorescence in the first 10 s:

$$peak\,\frac{\Delta F}{F_0} = \frac{\max\left(F_{stim}(t) - F_{bg_{stim}}(t)\right)}{\max(F_{pre-stim}(\mathrm{t}) - F_{bg_{pre-stim}}(\mathrm{t}))} - 1$$

Expression analysis

Gene expression was examined using transgenes with either the promoter fused to a fluorescent protein or the full gene product fused to a fluorescent protein. For *lite-1*$_{prom}$*::gfp, lite-1*$_{prom}$*::lite-*

1::gfp, *gur-3*$_{prom}$*::gfp*, *flp-15*$_{prom}$*::mCherry::gur-3*, and *prdx-2*$_{prom}$*::prdx-2::mCherry*, 40 optical sections (each 1 µm thick) were taken using a laser-scanning confocal microscope (Zeiss LSM 510), and a maximum axial projection was used to generate a single image.

RNA interference

Feeding RNAi was conducted as described (Timmons and Fire, 1998). Briefly, HT115 bacteria carrying the L4440 plasmid modified with sequences from the ORFeome library targeting *rft-1* and *rft-2* were spotted onto plates with IPTG. Clones were confirmed by sequencing. L4 larvae were transferred to RNAi plates, and their progeny were scored as adults as described above. L4440 without an insertion was used as the mock control.

SUPPLEMENTAL REFERENCES

Brenner, S. (1974). The genetics of Caenorhabditis elegans. Genetics *77*, 71-94.

Fang-Yen, C., Gabel, C., Samuel, A., Bargmann, C. and Avery, L. (2012). Laser Microsurgery in Caenorhabditis elegans. In Caenorhabditis elegans: Cell Biology and Physiology, J. Rothman, ed. (Boston: Academic Press), pp. 177-206.

Goodman, M., Hall, D., Avery, L. and Lockery, S. (1998). Active currents regulate sensitivity and dynamic range in C. elegans. Neuron *20*, 763-772.

Zimmer, M., Gray, J., Pokala, N., Chang, A., Karow, D., Marietta, M., Hudson, M., Morton, D., Chronis, N. and Bargmann, C. (2009). Neurons detect increases and decreases in oxygen levels using distinct guanylate cyclases. Neuron *61*, 865-879.